Pulsed NMR Experiment on Mineral Oil, $CuSO_4$ and Isoproponyl-2 samples

Herbert D. Ludowieg

Nuclear Magnetic resonance has been a tool that has been used by scientists for many years to analyze solids and liquids to identify structure and intrinsic properties of such materials. In this experiment, the Spin-Lattice relaxation time and Spin-Spin Relaxation time for mineral oil, copper sulfate solutions and Isoproponyl-2 were measured. The Spin-Lattice relaxation times of mineral oil and Isoproponyl-2 solution were measured to be: 37.7 ± 0.9 ms, 570 ± 30 ms respectively. The Spin-Lattice relaxation times of the CuSO $_4$ are as follows: 0.005M solution 99 ± 8 ms, 0.010M solution 61 ± 2 ms, 0.050M solution 13.6 ± 0.2 ms, 0.100M solution 6.5 ± 0.1 ms, 0.200M solution 3.26 ± 0.06 ms, 0.500M solution 1.25 ± 0.03 ms, 1.000M solution 0.69 ± 0.01 ms. For the Spin-Spin relaxation times of mineral oil the results are as follows: 58.2 ± 0.4 ms with individual measurements, 27.1 ± 0.9 ms with Carr-Purcell method and 54.8 ± 0.4 with the Meiboom-Gill method. For Isoproponyl-2 the Spin-Spin relaxation time was measured to be 174 ± 3 ms with the Meiboom-Gill method. For the $CuSO_4$ solutions the Meiboom-Gill method was employed and the Spin-Spin relaxation times are as follows: 0.005M solution 98 ± 3 ms, 0.010M solution 79 ± 1 ms, 0.050M solution 17.3 ± 0.6 ms, 0.100M solution 9.6 ± 0.3 ms, 0.200M solution 4.5 ± 0.1 ms, 0.500M solution 1.74 ± 0.05 ms and 1.000M solution 0.93 ± 0.02 ms.

I Introduction

Nuclear Magnetic Resonance (NMR) is a spectroscopic method that was developed by Edward Purcell and Felix Bloch independently with different instrumentation in the late 1940's. This new spectroscopic technique made use of the nuclear magnetic moments of atoms to be able to tell structure among other intrinsic properties of solids and liquids. This discovery marked a landmark in the study of materials by many different disciplines in scince including: physics, chemistry and biology.

Originally the method was developed with taking measurements of the Free Induction Decay (FID) signal. This was a signal that could be measured when a population of spins aligned in a magnetic filed given by a permanent magnetic field (B_0) were disturbed from that position along the z-axis by a Continuous Wave (CW) Radio Frequency (RF) magnetic field (B_1) along the xy-plane of the sample spins. The decay of the spins back to their equilibrium position along the z-axis became known as the FID signal. By analyzing this signal different properties of the material being tested would be found such as the Spin-Spin and the Spin-Lattice relaxation times.

However, in 1950 Edward L. Hahn had discovered that after the sample spins were excited by the B_1 pulse there would be a secondary pulse on the FID signal at resonance. It was noticed that this secondary would not be in response to the previous pulse which was a strong RF pulse lasting for a given amount of time. This would be known as the Hahn Spin Echo. This method has become widely used and is the basis for the measurements in this experiment.

NMR has also made its way into medicine in Magnetic Resonance Imaging (MRI) where it has offered a better alternative of imaging tissues by utilizing ions and other substances that can be imaged with NMR. It has become a better alternative since there is no longer the requirement of a radioactive sample being injected into the patient like in CAT scans where the patient is exposed to X-Rays. The only downside is that there can be no magnetic materials present or it can damage the high magnetic field magnet or the patient.

For this experiment a spectrometer designed by Teach-Spin will be used for the PNMR spectra. Specifically the PSA-1 spectrometer which includes all the necessary components for the experiment.

II Theory

NMR experiments can actually work because much like electrons, nucleons (protons, neutrons) have spin $\pm 1/2$ and arrange themselves in a configuration called the Nuclear Shell model which is depicted in a very similar fashion to that of the Atomic Shell model which describes the arrangement of electrons in the electronic orbitals. This is to say that they too fill up their respective shell positions according to the Pauli Exclusion principle. By having a very strong permanent magnetic field B_0 the nuclear spins could be alinged in the direction of the magnetic field (z-axis). With magnetic energy given by,

$$U = -\vec{\mu} \cdot \vec{B}[2] \tag{1}$$

Where, $\vec{\mu}$ is defined by,

$$\vec{\mu} = \gamma \hbar \vec{I}[2] \tag{2}$$

Where, $\vec{J} = \hbar \vec{I}$ is the angular momentum and $\vec{\mu}$ is the magnetic moment of the particle. With γ being the gyromagnetic ratio, $\vec{I}$ is the spin of the particle which is $\pm 1/2$ in our case. Therefore, the energy difference between the two energy levels becomes,

$$\Delta U = \hbar \omega_0 = \gamma \hbar B_0[2] \tag{3}$$

Where, B_0 is the permanent magnetic field aligned with the z-axis and $\omega_0 = \gamma B_0$ which gives the resonance

value for a proton. In which the gyromagnetic ratio is equal to $2.675 \cdot 10^4 rad/s \cdot gauss$ [2].
According to equation 3, the difference in the energy of the two spins is highly controlled by the permanent magnetic field that is used. Therefore, the energy difference between the two spins is very small and there is an almost equal probability of the spins being in one direction or the opposite when in the magnetic field. The Boltzman Distribution gives us the ratio of the spin populations as such,

$$\frac{N_1}{N_2} = e^{\frac{-\Delta U}{kT}} = e^{\frac{-h\omega_0}{kT}} [2] \quad (4)$$

Where, there will be a net spin population of approximately 1 in 10,000 in any of the directions. This is one reason for which NMR requires high number of nuclei present in the sample[1]. However, it's almost as likely that they will line up against the B $_0$ since the difference between the spin 1/2 and spin -1/2 are only a few milicalories apart. For this fact there is a thermal equilibrium of the two spin populations which follows the Boltzman distribution law. Which tells us that the population difference between these two states is less than 1 nucelus in 10,000. According to this, a very large sample will be needed in order to be able to make good measurements with NMR[1].
The fundamental principle behind NMR centers on the induction of the transition between the different Zeeman splitting levels of a nucelus. These splitting levels are important since they are the excited spin states of the nucleons and as they relax back to their ground state configuration they will create the FID signal. To be able to transition between the different spin states an additional field to B_0 must be applied. This field unlike the B_0 field must be a variable radio frequency (RF) field known as the B_1 field and it must have a frequency equal to the resonant frequency of the nucleons in the sample. It should also be noted that the transitions obey the transition rules of the angular momenta, that is to say, the difference in the angular momenta between the transitions cannot exceed 1 [2].

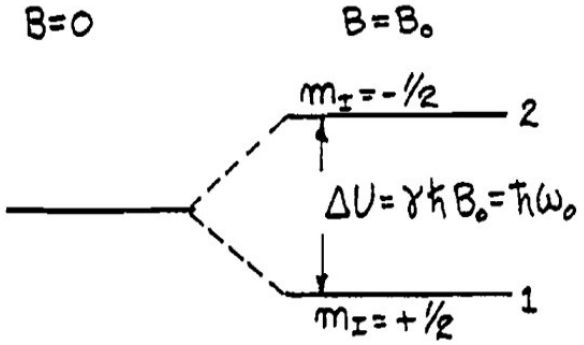

Figure 1: Zeeman splitting levels under presence of B_0 field[2].

Figure 1 gives a representation of the energy splitting in the different spin levels in a nucleus with spin $\pm 1/2$. However, there can exist a different number of spin states in different atoms depending on their total spin like in atoms with a total spin of 3/2. In figure 1 the energy splitting level is equal to the enrgy representation in equation 3.
The magnetization of the nuclei in the sample can be given by the following equation,

$$M_z = (N_1 - N_2)\mu [2] \quad (5)$$

Which is to say that this equation stems directly from the initial hypothesis that there is a correlation between the net spin populations in the sample and the magnetization of the sample. So then the expression to give the thermal equilibrium magnetization of the sample can be given by,

$$M_0 = N\mu \tanh(\frac{\mu B}{kT}) \approx N\frac{\mu^2 B}{kT} [2] \quad (6)$$

Where, N is the difference between the spin states. It should be noted that this thermal equilibrium magnetization is not instantaneous. Though, nothing is instantaneous; nothing can be faster than the speed of light. This property is time dependent and it grows in an exponential fashion as represented of Figure 2. The differential equation that describes the process of rate of aproach to thermal equilibrium is give by equation 7.

$$\frac{dM_z}{dt} = \frac{M_0 - M_z}{T_1} [2] \quad (7)$$

In which, T_1 is the Spin-Lattice relaxation time. This property is a property which is different between samples and describes the lifetime of a nucleonic spin in an excited state before relaxing back to its thermal equilibrium position. By which, may be one extremely important factor in an experiment since were it not for the spins re-establishing thermal equilibrium the experiment would not be able to continue. The Spin-Lattice environment is defined by the Spin reffering to the individual nucleonic spin that is being measured and the Lattice which includes the entire surroundings of the nuceleons. By integrating equation 7 we get to equation 8 which relates the exponential decaying of the measurable magnetization, which can only occur in the xy-plane, to the Spin-Lattice relaxation time [1].

$$M_z(t) = M_0(1 - e^{-t/T_1}) [2] \quad (8)$$

As it has been stated the T_1 time depends on the material being tested and can have a very wide range which can range from milliseconds to seconds [2]. Since this property gives the amount of time that will take for the system to re-establish equilibrium. One must give this much time in between repetitions of measurements to be able to take correct measurements or else the spins may be in an excited state and never give useful data.
Now, one should keep in mind that this is the very basic concepts behind the Spin-Lattice phenomena. The other forms of Relaxation Phenomena related to Spin-Lattice relaxation may come into play when delaing with organic molecules and multi-species samples. Some of them are: Dipole-Dipole Relaxation,

Spin-Rotation Relaxation, Chemical Shift Anisotropy and Scalar relaxation. These are believed to be outside the scope of this report so they will not be explained [1].

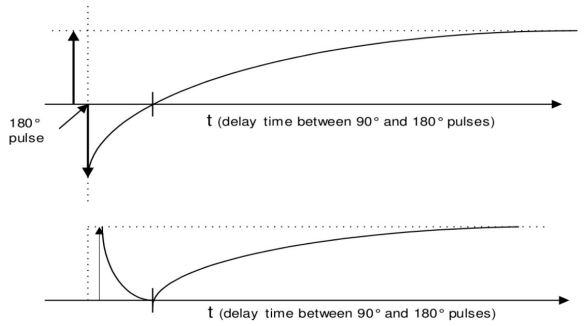

Figure 2: Upper trace: graphical representation of the relaxation of the spins after exriencing a 180° pulse. The intersection with the x-axis gives the Spin-Lattice relaxation time. Lower trace: measured representation of the spins during the experiment. Note the initial decay as compared to the upper trace.

As is mentioned in the caption on Figure 2 one method to get the T_1 relaxation time is by finding the intersection on the x-axis. Now here comes the problem, by inspection of equation 8 there will be a problem when trying to solve the equation for 0 analytically. The steps one can take are the following.

$$\begin{aligned} M_z(t) &= M_0(1 - e^{-t/T_1}) \\ 0 &= M_0(1 - e^{-t/T_1}) \\ 1 &= e^{-t/T_1} \\ \ln 1 &= \frac{-t}{T_1} \\ 0 &= \frac{-t}{T_1} \end{aligned}$$

In which, the very last line presented makes no mathematical sense since t/ T_1 will not be zero unless t = 0. To combat this an error term, ϵ, is added by splitting equation 8 to look like,

$$M_z(t) = (M_0 + \epsilon) - M_0 e^{-t/T_1}) \tag{9}$$

Where the first term will be represented as one whole number in the discussion section. However, there is another method that can also be used. By simple inspection of equation 8, once again, one can see that the value of interest is contained in the exponential term, for which one could in fact, make use of the fact that the data will have an exponential fit and use the exponential term to calculate the T_1 relaxation time. The accuracy of these two will be compared and discussed further in the Discussion section.
There exists a second form of relaxation different to that previously introduced, Spin-Spin Relaxation time (T_2). While the T_1 process describes the transfer of energy from a spin into the environment, the T_2 process describes the loss of phase of a system over time [3]. This dephasing is usually due to neighboring spins that interact with each other and since they themselves have a magnetic moment they will make an inhomogenous magnetic field on a microspcopic scale. Due to these inhomogenieties in the magnetic field the individual magnetic moments will precess at different frequencies [1]. This type of relaxation is only present when the proper B_1 field is applied on the sample inducing a rotation of the magnetic momenta. Which then leads to the precession of the spins about the B_0 field. This secondary magnetic field B_1 is actually a circularly polraized magnetic field which can be represented by the equation,

$$\vec{B} = B_1 \cos(\omega t)\hat{i} + B_1 \sin(\omega t)\hat{j} + B_0\hat{k}[2] \tag{10}$$

Due to the fact that this is a rotating magnetic field about z-axis it is useful to make a stationary frame with respect to the B_1 field. Then the equation for the net magnetic field on the atom is,

$$B^*_{eff} = B_1\hat{i^*} + (B_0 - \frac{\omega}{\gamma})\hat{k^*}[2] \tag{11}$$

Where the new coordinate axes are shown on Figure 2.

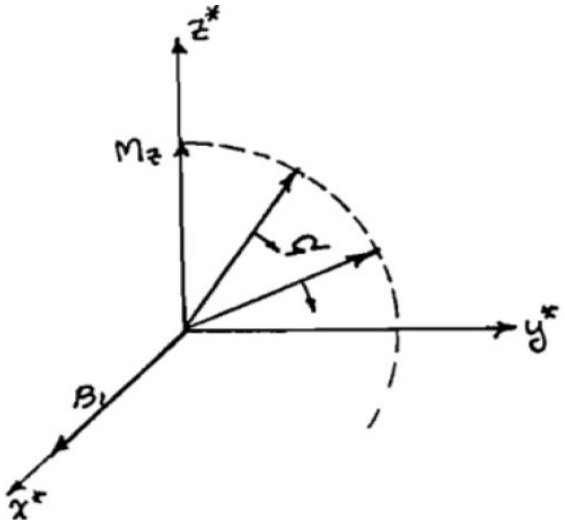

Figure 3: Rotating frame coordinates with M_z precessing with angular velocity Ω [2].

The equation that will describe the motion of the spins in the Magnetic field is given by equation 12.

$$\frac{d\vec{M}}{dt} = \gamma\vec{M} \times B^*_{eff}[2] \tag{12}$$

The rotation of the M_z field is equal to γB_1.
One of the most important concepts in PNMR that describes it as being pulsed is the use of strong RF pulses. They are exactly the ones that were introduced before with Hahn Spin Echo. There are three main different types of pulses that need to be introduced: 90°, 180° and 360°. The pulses are known under this convention because they give the angle by which the angular

momenta are displaced from their position prior to the pulse being applied. That is to say when the 90° pulse is applied on the system the angular momenta may shift from the z-axis to the xy-plane. If the 180° pulse is applied to the system the angular momenta shift from the z-axis to the -z-axis. All of these pulses have the exact same conditions except for the length of time by which they are applied. As such, the length of time that is needed by different materials may vary. The role that this has on the experiment is that as long as the spins are aligned with the z-axis measurements cannot be taken. Only when they are shifted to the xy-plane will they be able to give an FID signal and become measurable by the instruments. Due to the T_1 relaxation time the magnetization along the xy-plane will not hold for a very long amount of time and decay exponentially. This is represented on the figure below.

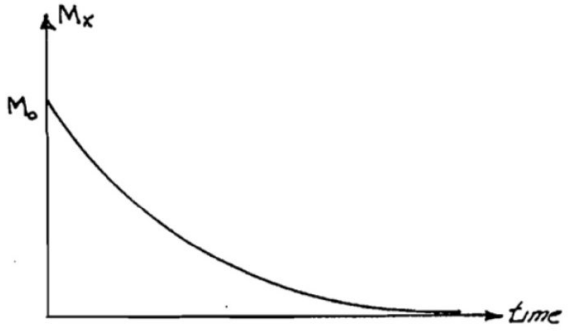

Figure 4: Exponential decay of the Magnetization in the xy-plane as a function of time [2].

So far, anything that has to do with the PNMR experiment has been largely dominated by the Spin-Lattice relaxation time. Now, let's see where the Spin-Spin relaxation time comes into play. Previpously it has been mentioned how the Hahn Spin Echo can appear without having a previous excitation from any RF pulse. Well this is actually due to the precessing spins on the xy-plane. The Hahn Spin Echo technique can be employed to measure the Spin-Spin relaxation times and the method makes use of a singular 90° pulse followed by a after some time constant, τ, a 180° pulse. The importance of this sequence is that by pulsing with a 90° pulse the spins will be shifted from the thermal equilibrium axis to the xy-plane where after the time constant they will have precessed according to their Spin-Spin relaxation time. Now it is important to note that, the spins will split approximately half going one way and half the other way [1]. Also, the spins they do not all precess at the same rates. Some will be slower than others.
By applying the second pulse, 180°, the spins will flip on the xy-plane and continue to precess at their same rates and directions. Which means then, that the slower spins will be ahead of the faster precessing spins in the hope that they all come back and meet in the same place. As they precess the spins point in random directions and can be approximated to cancel each other out. It is only when they re-phase with one another that the Hahn Spin Echo signal can be viewed. A pictoral representation of this is shown on the figure below.

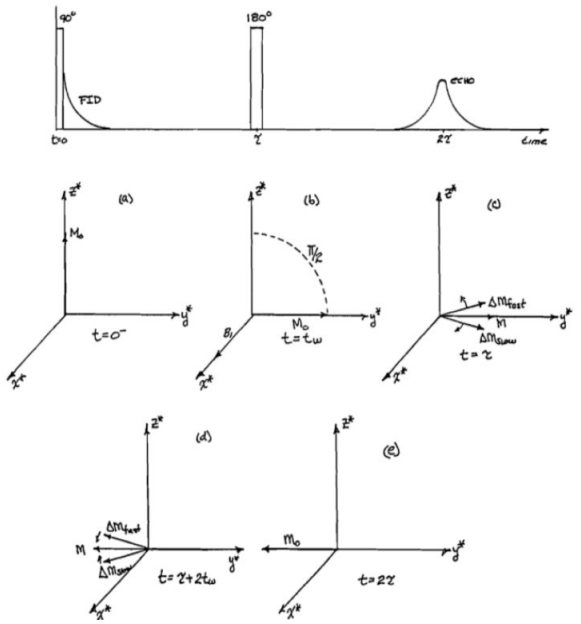

Figure 5: Top Figure: representation of the signal received from the instruments. (a) Initial state at thermal equilibrium. (b) A strong 90° RF pulse is applied on the system at resonance; the angular momenta shift to the xy-plane. (c) Angular momenta begin to precess on the xy-plane due to the Spin-Spin interactions. (d) A strong 180° RF pulse is applied and flips the angular momenta on the xy-plane. (e) Spins regain phase and give rise to the peak at time (2τ) [2].

However, the amount of time for which the spins are allowed to freely precess must be less than the Spin-Lattice relaxation time. Otherwise the spins will re-establish thermal equilibrium and applying a 180° will not achieve any measurements. That is to say that the longer the τ value the lower the peak heigth of the Hahn Spin Echo. The equation relating the Spin-Spin relaxation time to the magnetization along the xy-plane is the following,

$$M_{x,y}(2\tau) = M_0 e^{-2\tau/T_2} [1] \tag{13}$$

Finally, one last mention that the above theoretical model is best applied on single nucleonic spins. When molecules are to be studied and even some larger atoms the magnetic field will be different due to the induced orbital motions of the electrons in the orbitals. Even the diamagnetic moment of some nearby atoms and molecules can greately affect the Larmour frequency of the nucleus being examined [1].

III Experimental Set-Up

As it was mentioned before, for this experiment Teach-Spin's PS1-A spectrometer will be used. Figure 6 and 7 are a simplified block diagram of the set-up.

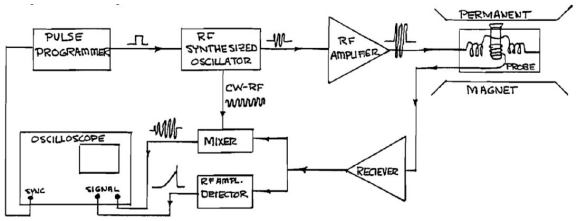

Figure 6: Simplified block diagram of the entire experimental set-up [2].

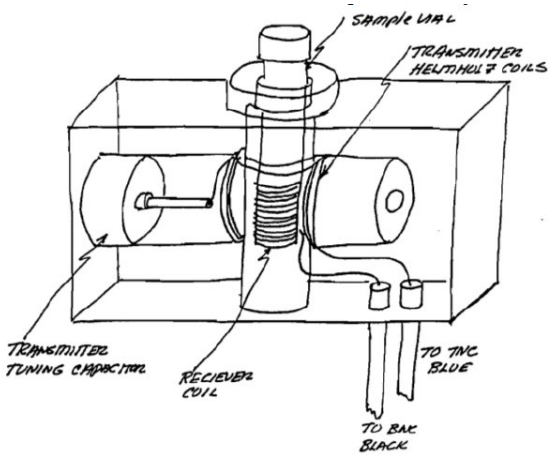

Figure 7: Close-up of the Magnet Diagram including the permanent magnet, receiver coils and the coils giving off the RF magnetic field [2].

The coils giving off the B_1 are arranged in a helmholtz configuration to provide maximum field homogeneity to the sample. On Figure 6 the cycle starts from the oscilloscope, where the resonant frequency for the sample is set and sent to the pulse programmer. The pulse programmer takes care of transforming the input into the specific pulses. Whose width depends on the values that the knobs are set to, the knobs will be pointed out later. From there it moves through the rest of the circuit to the sample. going thorugh the wires and creating the RF fieldi [2].
Figures 8 and 9 show the controller unit that houses all the modules to perform the experiment and the magnet with the probe housing respectively.

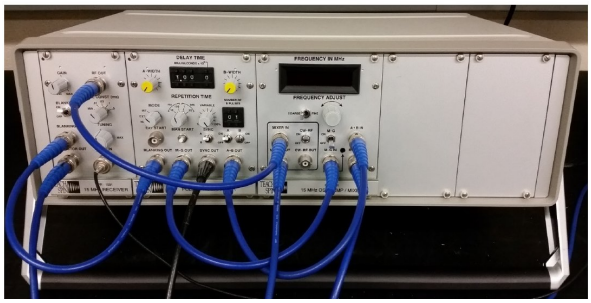

Figure 8: Controller Unit the last two modules are empty for further expansions [2]

Figure 9: Magnet Assembly housing permanent magnet and sample holder [2].

The detector coil has two different outputs, one which goes to the mixer and one that goes to the detector out port on the controller unit. The mixer on the block diagram takes the frequency that is to be inputted into the coils and mixes it with the output of the detector. This will be important to remember for the actual experiment. The resonant frequency will be achieved when the beat output on the oscilator from the mixer output is nearly zero.
The magnetic field due to the permanent magnet ha sbeen measured at the factory and all of the specs for the magnet will be included at the end of this section. The plastic cover that is on the magnet housing should be kept there when there is no need to immediately access the sample for any source of magnetic field could degrade the homogeneity of the field. Also, the magnets can be brittle so be careful with metal that is close to the magnet [2].
This magnet like many others is temperature depen-

dent. However, since the temperature under which the magnetic field of the magnet was measured is unknown the following equation would not be of much use in calculating the resonant frequency.

$$\Delta H = 4gauss/^oCor17kHz/^oCforprotons \qquad (14)$$

There is a proportional relationship between the temperature of the magnet and the field strength. The temperature of the magnet should be kept as cool as possible to avoid too much drifting in the resonant frequency. It is very possible that it will need to be checked quite periodically in order to maintain the resonance condition [2].
The pulse programmer is shown on Figure 10 and it is a complete self-contained pulse generator. The controls are as follows:
A-Width: Width of A pulse between 1-30 μs.
B-Width: Width of B pulse between 1-30 μs.
Delay Time: Delay between the A and B pulses. Can be set to any number between 0.01 to 9.99e3 ms.
Accuracy: 1 pt in 10^6 on all delay times.
Mode: Int (Internal): The pulse stream is repeated with a repetition time selected by the two controls on the right of the mode switch.
Ext (External): the pulse stream is repeated at the rising edge of an external TTL pulse.
Man (Manual): the pulse stream is repeated every time the manual start button is pushed. this allows the experimenter to choose arbitrarily long repetition times for the experiment.
Repetition Time: Sets the interval in between each measurement taken. The variable node next to it sets what percentage of it will be the value.
Number of B pulses: Number of B pulses from 0 to 99

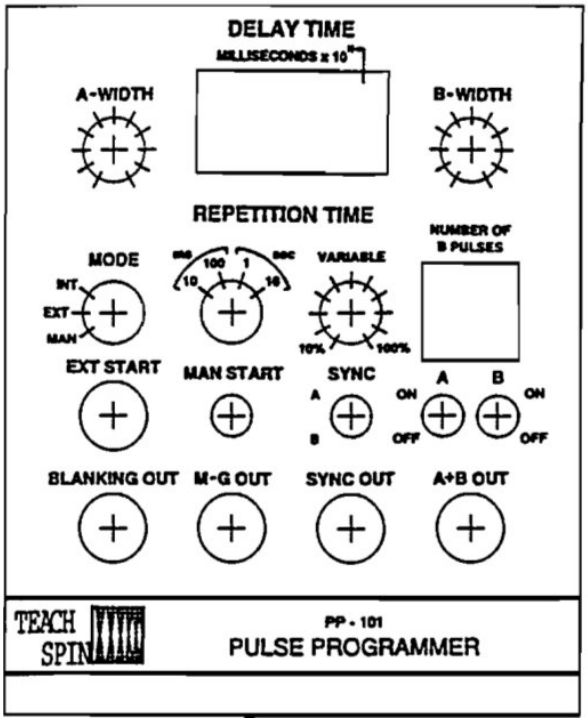

Figure 10: Pulse Programmer [2].

IV Results and Discussion

(i) The Spectrometer
For this part of the experiment just had to hook up all of the cables according to the picture given, figure 11.

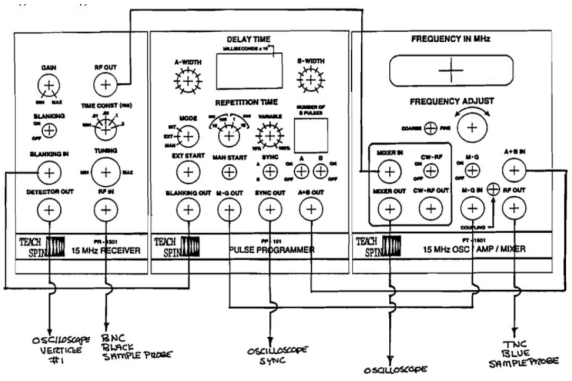

Figure 11: Gives the schematics for which cables are supposed to go where.

(ii) Pulse Programmer

For this section of the experiment just had to play with the pulse programmer and get aquaited with what all of the knobs and other buttons did. As expected when the scale settings for the time were changed the pulse got smaller and larger depending on which way we go with the scale. When the repetition variable scale was changed from 10% to 100% there

was a change in the amplitude of the pulse.

(iii) Pulse-Sequences

As we changed the width of the pulses there did not seem to be much of a change. Looking back on it there may have been some errors made since nothing was seen to happen in terms of the spin echo. One possibility was that it was so far out of resonance that the spins never had enough of a precession to be able to create a strong enough signal to be able to see noticeable changes. Also, there was the problem of what to look at.

(iv) Multiple Pulse Sequences

In this part of the experiment we began to test what the Carr-Purcell and Meiboom-Gill method that would later be used would look like. As the number of pulses was increased all that seemed to increase was the number of pulses. Pulse width was the same for all, the B pulses but amplitude was the same.

(v) The Receiver

For this part of the experiment the resonant frequency had to be found experimentally. By using equation 3 we could approximate the resonant frequency to approximately 14.903 MHz when we adjusted it experimentally we found that in the position that we were currently in it was more around 15.422 MHz. I mention the current position since we would later go ahead and map out the magnet to find areas of uniformity and the frequency varied between the different areas in the magnet.

(vi) Single Pulse NMR Experiment - FID
In this part of the experiment we were trying to get a FID signal from one single 90° pulse at resonant conditions. Figure 12 shows our result for this part of the experiment.

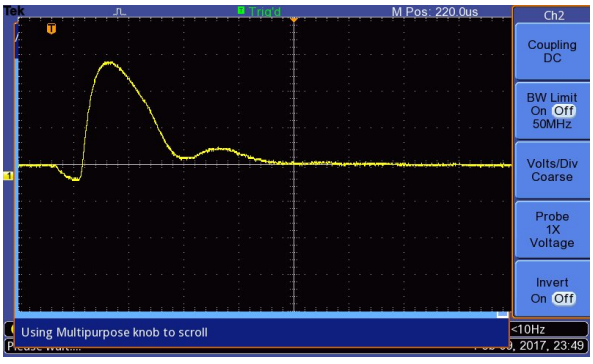

Figure 12: Signal from the RF amplifier detector.

(vii) Magnetic Field Contours

In this part of the experiment we tried to find the "sweet spot" of the magnet where the field would be most uniform. The importance of this is that we don't want a field which is not constant since then there is a posibility that the spins of the nucleons won't align themselves as well as they should if at all. For this part we chose to have a grid with a resolution of 0.5 units in the horizontal direction from -3 to +3 and a vertical resolution of 1.0 units from 10 to 20 units. This in turn gave us a plot that looks like figure 13. With the use of this figure it was determined that the "sweet spot" of the magnet would be at approximately 13 units in the vertical and -0.75 units in the horizontal. With an experimentally determined resonance value of 15.43 ± 0.02 MHz. We determined this error because from the RF coils the variance can be 17 kHz/ °C. So it seems within reason to assume that the resonance would drift by more than that of 1°C.

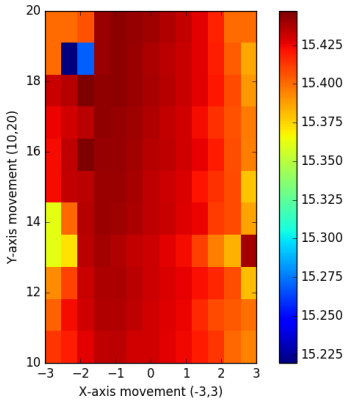

Figure 13: 2D colorplot of the magnet homogeneity gotten using python.

(viii) Rotating coordinate systems

It was determined that by using the channel 1 input of the oscilloscope the positions of the different pulse widths could be determined where the first 90° pulse was the first maximum from the minimum pulse width, 180° is the first minimum after the first maximum and so on.
The reason for this is that at the 90° the magnetization is pushed fully to the xy-plane and therefore has the greatest signal since we can only measure the signal in the xy-plane. At 180° the magnetization is pointing along the -z-axis so it is almost the same as it being along the z-axis and there will not be any measuarable signal.
It is not possible to create a total angular shift in the spins simply because it does not have the necessary energy to be able to cause the Zeeman transition into the excited that causes the spin to give off the signal as it relaxes.
(ix) Spin Lattice relaxation time T_1

In this part of the experiment the Spin Lattice relaxation of mineral oil was found with two methods. The first was a sort of guess to approximate where to expect the zero for the data that we would take with the second method. For the second method screenshots of the oscilloscope were taken to collect the data of the spin magnetization when undergoing a 180° - τ - 90° pulse sequence. Where τ is the delay time in milliseconds.
With the first method we approximated the value to 38 $\pm$ 2 ms. The error was chosen as such due to the fact that within those two milliseconds there was very little noticeable change in the height of the peak. So, it became hard to determine the actual time.
When using the data we got a value 37.7 $\pm$ 0.9 ms with an exponential fit using the curve_fit tool in Python to fit to the fit equation $y = -Ae^{-kx} + B$. Where, x and y where the data points and all the rest were fit parameters. When we used the other method discussed in the theory section we got a value that when used in the actual experiment did not match up. The exponantial fit of the data is shown of figure 14.

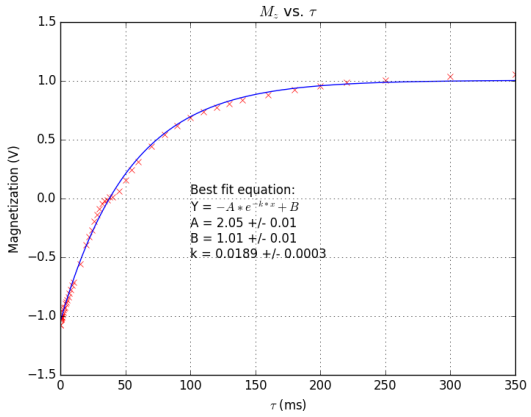

Figure 14: Exponential fit of data gotten to calculate the spin-lattice relaxation time of mineral oil.

(x) Spin-Spin relaxation time

In this part of the experiment we used three different methods to find the Spin-Spin relaxation time of mineral oil: individual echo measurement, Carr-Purcell method and Meiboom-Gill method. For which we got values of 58.2 $\pm$ 0.4 ms, 27.1 $\pm$ 0.9 and 54.8 $\pm$ 0.4 ms respectively. From the results it is clear that the other two methods completely outdid the Carr-Purcell method. The weakness in the Carr-Purcell method is that is the 180° pulses are only a few degrees off it can really add up significantly as more and more pulses are observed dephasing the spins ever so slightly until they all point in random directions and the signals cancel themselves out.
The plots of the exponential fits use the fit equation $y = -Ae^{-kx}$. Where, x and y are the data and A and k are the fit parameters.

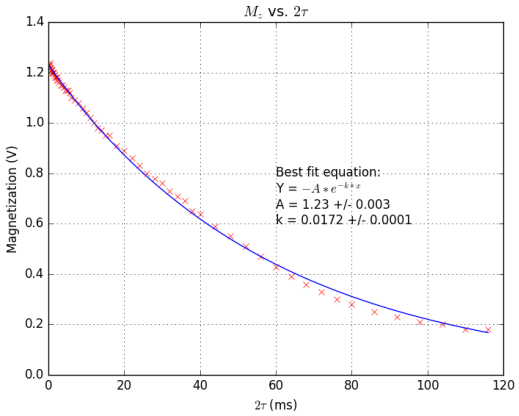

Figure 15: Mineral oil T2 with individual spin echo measurements.

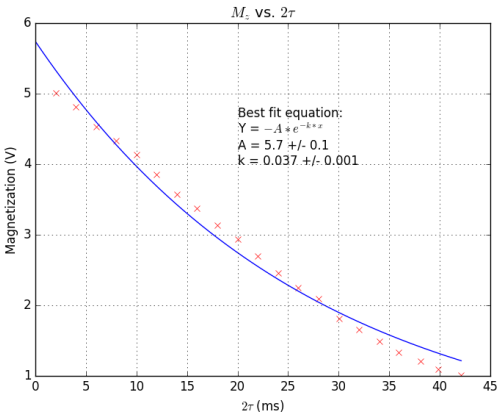

Figure 16: Mineral oil T2 with Carr-Purcell method.

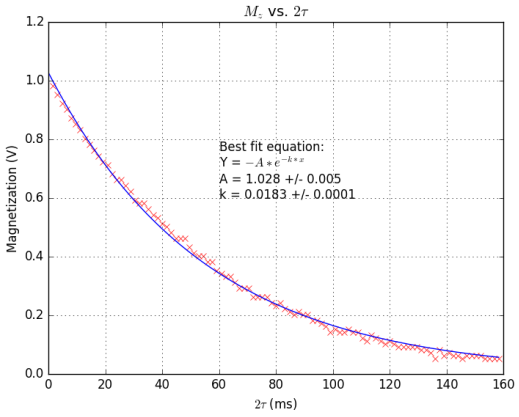

Figure 17: Mineral oil T2 with Meiboom-Gill method.

(xi) $CuSO_4$ solutions

In this part of the experiment we measured the Spin-Lattice and Spin-Spin relaxation times for 5 different

solutions of Copper(II) Sulfate: 0.005M, 0.010, 0.050M, 0.100M, 0.200M, 0.500M and 1.000M. The values for the relaxation times are shown in the following table.

(M)	T_1	T_2	$1/T_1$	$1/T_2$
0.005	99 ± 8	98 ± 3	0.0101	0.0102
0.010	61 ± 2	79 ± 1	0.0164	0.0127
0.050	13.6 ± 0.2	17.3 ± 0.6	0.0735	0.0578
0.100	6.5 ± 0.1	9.6 ± 0.3	0.1538	0.1042
0.200	3.26 ± 0.06	4.5 ± 0.1	0.3067	0.2222
0.500	1.25 ± 0.03	1.74 ± 0.05	0.8000	0.5747
1.000	0.69 ± 0.01	0.93 ± 0.02	1.4493	1.0753

The exponential fit functions are identical to those of the mineral oil.

There was a direct relationship between the molarity and the $1/T_1$ and $1/T_2$ values. This makes sense because there are more copper spins present that will be able to be magnetized into the Zeeman splitting levels.

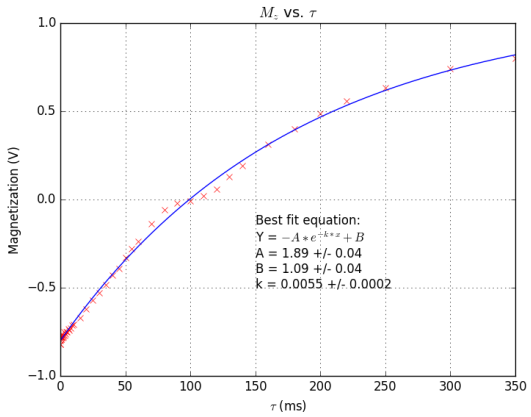

Figure 18: Spin-Lattice relaxation of 0.005M Copper(II) Sulfate.

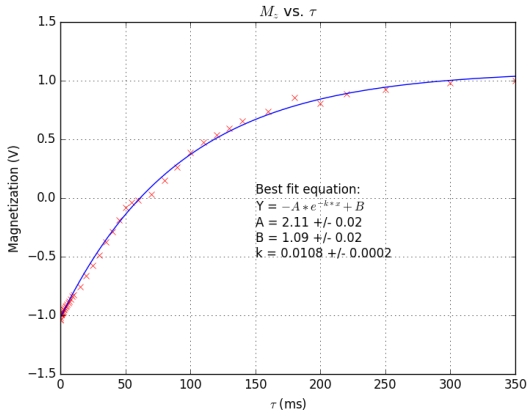

Figure 19: Spin-Lattice relaxation of 0.010M Copper(II) Sulfate.

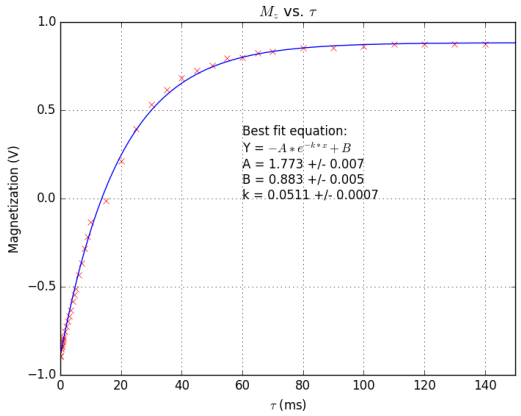

Figure 20: Spin-Lattice relaxation of 0.050M Copper(II) Sulfate.

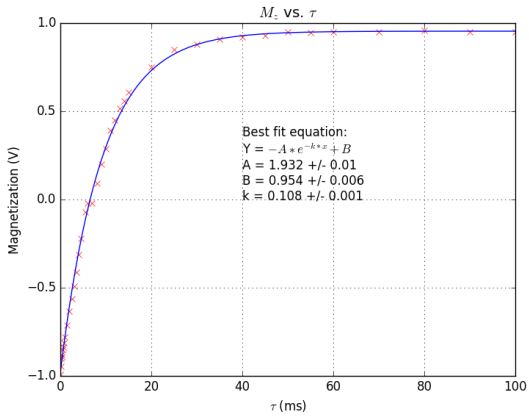

Figure 21: Spin-Lattice relaxation of 0.100M Copper(II) Sulfate.

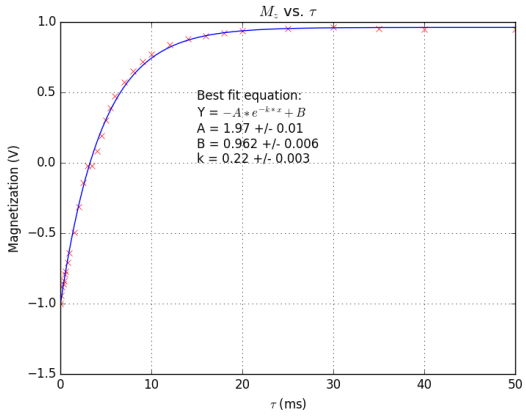

Figure 22: Spin-Lattice relaxation of 0.200M Copper(II) Sulfate.

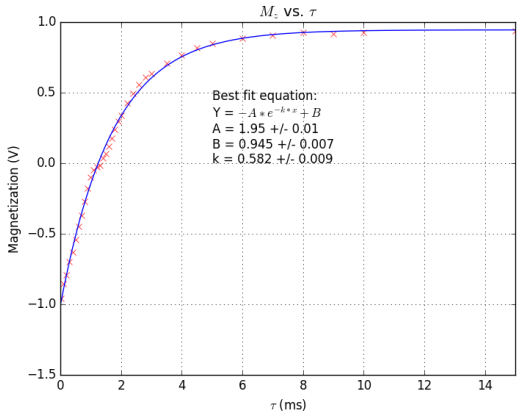

Figure 23: Spin-Lattice relaxation of 0.500M Copper(II) Sulfate.

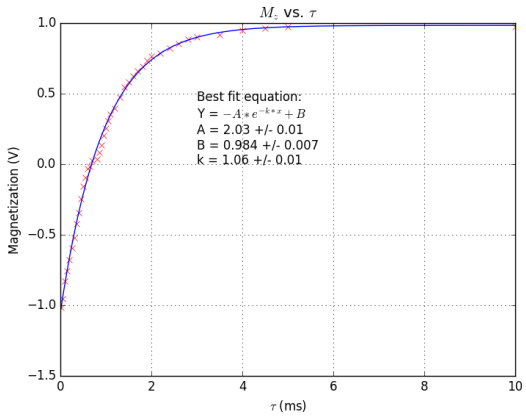

Figure 24: Spin-Lattice relaxation of 1.000M Copper(II) Sulfate.

For Spin-Spin Relaxation.

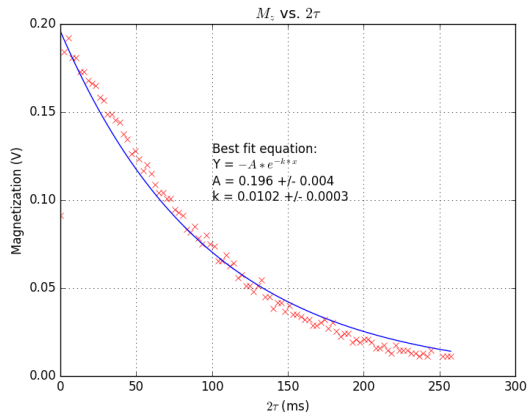

Figure 25: Spin-Spin relaxation of 0.005M Copper(II) Sulfate.

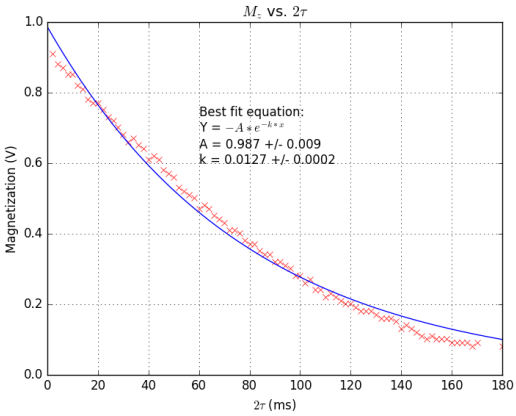

Figure 26: Spin-Spin relaxation of 0.010M Copper(II) Sulfate.

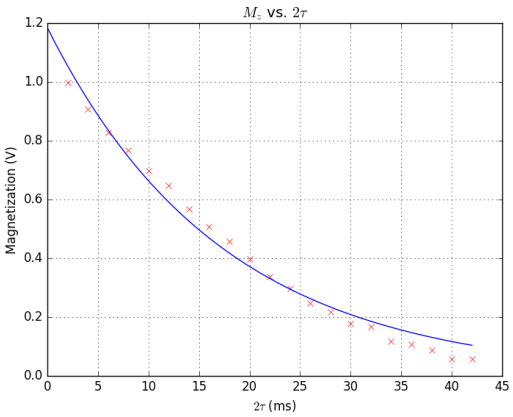

Figure 27: Spin-Spin relaxation of 0.050M Copper(II) Sulfate.

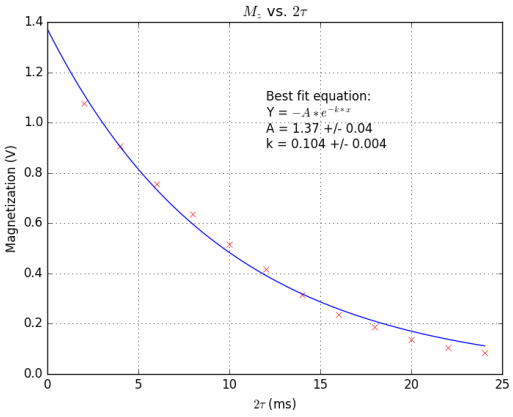

Figure 28: Spin-Spin relaxation of 0.100M Copper(II) Sulfate.

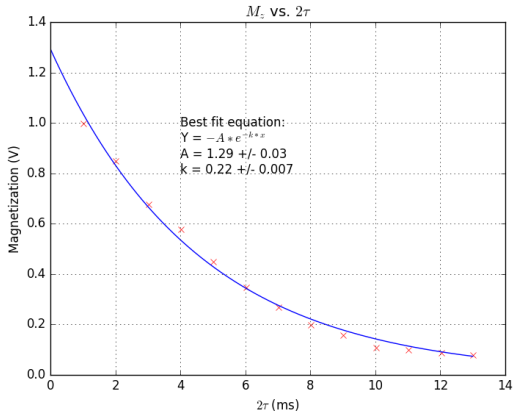

Figure 29: Spin-Spin relaxation of 0.200M Copper(II) Sulfate.

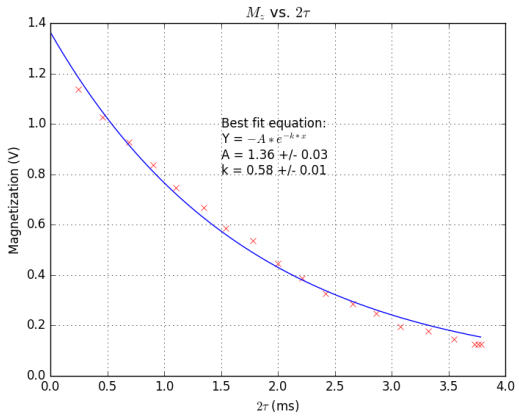

Figure 30: Spin-Spin relaxation of 0.500M Copper(II) Sulfate.

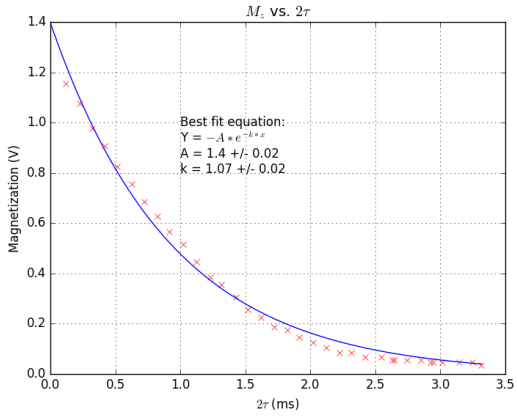

Figure 31: Spin-Spin relaxation of 1.000M Copper(II) Sulfate.

The Molar Concentration plots are the following.

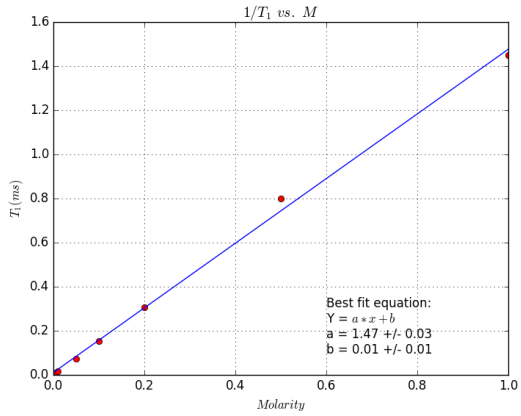

Figure 32: Spin-Latice relaxation time vs. MolariltyCopper(II) Sulfate.

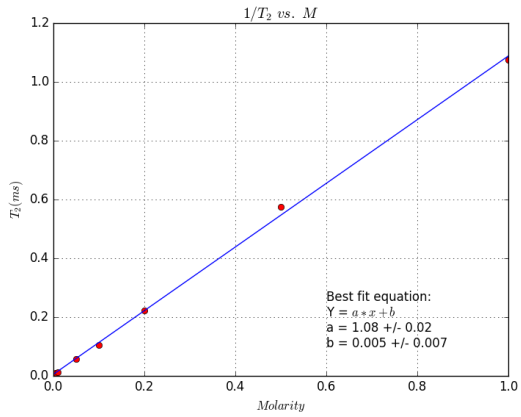

Figure 33: Spin-Spin relaxation time vs. Molarity Copper(II) Sulfate.

(xii) Natural Products

We chose Isoproponyl-2 alcohol as our natural product and got the values of 570 $\pm$ 30 ms for the Spin-Lattice Relaxation time and 174 $\pm$ 3 ms for the Spin-Spin relaxation time.

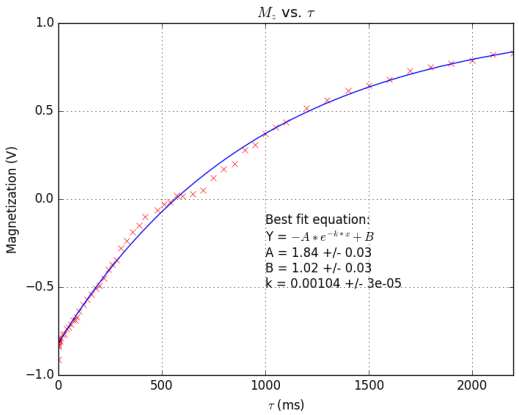

Figure 34: Spin-Lattice relaxation of Isoproponyl-2 Alcohol.

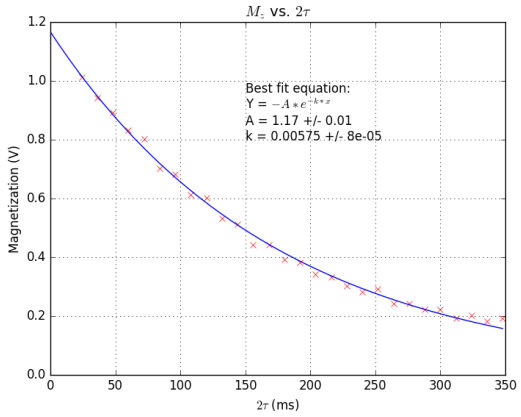

Figure 35: Spin-Lattice relaxation of Isoproponyl-2 Alcohol.

One of the possible reasons why our results for the alcohol are not as expected could be since it is an organic molecule it does have some extra factors that need to accounted for like those discussed at the end of the theory section.

V Conclusion

PNMR is an extremely useful tool that has been used and developed over the past decades. Recently there have been many advances into the nano-scale NMR at non-cryogenic temperatures through the use Nitrogen-Vacant Diamond centers which have been able to achieve resolutions equal to or better than those of methods that use cryogenic temperatures.

References

[1] Paudler, W. W. (1987) *Nuclear Magnetic Resonance General Concepts and Applications*. John Wiley & Sons Inc.

[2] PHY 408 Lab manual. *Pulsed NMR*

[3] Ratner, M. A.; Schatz,G. C. (1993) *Quantum Mechanics in Chemistry*. Englewood Cliffs, New Jersey : Prentice-Hall Inc.